fect is less significant because the fixed objects are farther from the edge of the traveled way. Therefore, underground placement is the best alternative for a greater number of fixed objects on street B.

The results shown in Figure 6 for 30 000 ADT show a similar best-alternative pattern. However, on street B, because of the higher annual accident costs, the effects of zero utility-pole accident costs by using underground placement are not offset as quickly with increased numbers of fixed objects. Thus, underground placement is the best alternative in all cases for 30 000 ADT on street B.

## CONCLUSIONS

The demonstration of the methodology presented above indicates its applicability to a variety of improvement alternatives and various traffic and roadside conditions. Also, it illustrates the sensitivity of the selection of the best improvement alternative to traffic and roadside conditions. However, generalization concerning the relative economies of the alternatives should not be made on the basis of these results. It must be remembered that these results were for only one vehicle size, one utility-pole spacing, and one other type of fixed object, which was assumed to have the same collision properties as the nonbreakaway utility poles. Again, the purpose of the demonstration was not to identify the best alternatives for all conditions but to show the applicability of the methodology and some effects of traffic and roadside conditions on the relative economies of the alternatives. Also, although not described in this paper, the demonstration was conducted with the aid of a computer program of the methodology, which obviously facilitated the computations.

Finally, it should be noted that meaningful results from the use of the methodology require that local unit cost data be used. The costs used in the demonstration will most likely not be appropriate for other times and other places. Also, in the presentation of the formulation of the methodology, the results of research on the nature and frequency of roadside encroachments and collision severities, which are used in the calculation of accident and collision maintenance costs, were included. Their inclusion was primarily for the purpose of showing the nature of these factors and how they are incorporated within the methodology. However, the integrity of the methodology would not be compromised if the values of these factors were modified in accordance with the results of more recent (or future) research. In fact, such modifications should be made as more knowledge is gained.

## REFERENCES


1. Cost-Effectiveness of Countermeasures for Utility Poles. Federal Highway Administration, U.S. Department of Transportation, June 1980.
2. E.R. Post, P.T. McCoy, and others. Feasibility Study of Breakaway Stub Concept for Wooden Utility Poles. Civil Engineering Department, Univ. of Nebraska--Lincoln, Res. Rept. TRP-03-005-79, Dec. 1979.
3. J.W. Hutchinson and T.W. Kennedy. Median of Divided Highways--Frequency and Nature of Vehicle Encroachments. Univ. of Illinois, Urbana-Champaign, Engineering Experiment Station Bull. 487, 1966.
4. J.C. Glennon and C.J. Wilton. Methodology for Determining the Safety Effectiveness of Improvements on All Classes of Highways. In Effectiveness of Roadside Safety Improvements, Rept. FHWA-RD-75-23, Federal Highway Department, U.S. Department of Transportation, Nov. 1974, Vol. 1-A.
5. H.E. Ross. Impact Performance and a Selection Criterion for Texas Median Barriers. Texas A&M Univ., College Station, TTI Res. Rept. 140-8, April 1974.
6. Institute of Traffic Engineers. Transportation and Traffic Engineering Handbook. Prentice-Hall, Englewood Cliffs, NJ, 1976.
7. E.R. Post and P.T. McCoy. Feasibility Study of Retrofitting Concrete Median Barriers. Civil Engineering Department, Univ. of Nebraska--Lincoln, Res. Rept. TRP-03-006-80, May 1980.
8. E.R. Post, R.J. Ruby, P.T. McCoy, and D.O. Coolidge. Cost-Effectiveness of Driveway Slope Improvements. TRB, Transportation Research Record 685, 1978, pp. 14-19.


*Publication of this paper sponsored by Committee on Safety Appurtenances and Committee on Utilities.*

*Abridgment*

# Loads on Bridge Railings

JAMES S. NOEL, T.J. HIRSCH, C.E. BUTH, AND A. ARNOLD

**Recent and ongoing research studies have addressed the problem of improving the performance of bridge-railing systems and extending the range of vehicles that can be restrained. This paper summarizes the results of one of these studies. A series of full-scale crash tests was completed that used several representative vehicle geometries and weights and an instrumented concrete barrier. The measured resultant loads, locations, and distributions are tabulated and discussed. Because the wall is relatively rigid—at least in comparison with most bridge railings—it is an obvious conclusion that the reported force magnitudes represent an upper limit. They are expected to be considerably smaller for collisions with more-compliant barriers. An equal corollary is that the contact duration will be longer.**

The American Association of State Highway and Transportation Officials (AASHTO) Standard Specifications for Highway Bridges (1) sets forth design requirements for bridge railings. These requirements include limits on certain geometrics and set forth design loads. The basic load is a 10-kip static force applied at any location along the longitudinal axis of the railing; the vertical distribution depends on the railing configuration. The specifications further require that elastic structural analysis and design procedures be employed.

These requirements are intended to produce bridge-railing designs that will function adequately for most traffic conditions that involve full-sized automobiles; the reserve load capacity of the railing, besides its elastic strength, offers some degree of protection for heavier vehicles such as school buses.

Characteristics of the vehicle population are changing. The advent of the smaller, subcompact automobile and its increasing popularity present new considerations to the designer of bridge railings. Also, recent catastrophic accidents that involved large vehicles have brought about an increased awareness of a need to provide better protection for these vehicles. Several recently completed and ongoing research studies have addressed the question of design requirements and performance standards for bridge railings. This paper presents a portion of the results from one of these studies.

An instrumented concrete wall designed specifically to measure the magnitude and location of vehicle impact forces was constructed. The relatively rigid wall, as shown in Figure 1, consisted of four 10-ft-long concrete panels each supported by four link-type load cells. Each of the massive panels (42 in high and 24 in thick) had an accelerometer to account for inertia factors. Surfaces that made contact with adjacent panels (and the supporting slab) were Teflon coated to minimize friction. A simple computer program was used to calculate force magnitudes and locations panel by panel from the electrical outputs. A static calibration of the system provided the correspondence factors required by the computer program. The results were successfully confirmed by using a dynamic calibration that involved a large mass and contact pad.

Eight actual full-scale impact tests were completed: two used subcompact 1800-lb sedans, two used compact 2250-lb sedans, two used full-sized 4500-lb sedans, one used a 66-passenger 20 000-lb school bus, and one used a two-axle 32 000-lb intercity bus. In most of the tests, the angle of impact was 15°; however, in two tests, it was more than 20°. Vehicle speeds in all tests were near 60 mph.

The results of these tests were measured and recorded on magnetic tape and on film. These data were analyzed to determine the resultant magnitudes, locations, and distributions of the contact forces. Once the time-changing magnitudes and locations of the resultant forces on the four instrumented wall segments during each collision are known, it is necessary to make judgments concerning the distributions of the contact (or bearing) stresses.

The first of these judgments concerned how to handle force spikes and other rapidly changing phenomena observed from the instrumented-wall outputs. These spikes are of little consequence to the required structural integrity of bridge railings. Therefore, maximum forces were obtained by averaging the data over 0.05-s intervals. Two such 0.05-s intervals were inevitably appropriate for each of these tests--one for the initial impact of front fender, bumper, and wheel with the rail and one for the second, or final, impact as the rear of the vehicle rotates into the rail. Each 0.05-s increment was chosen to give the largest average resultant force.

**Figure 1. Instrumented wall.**

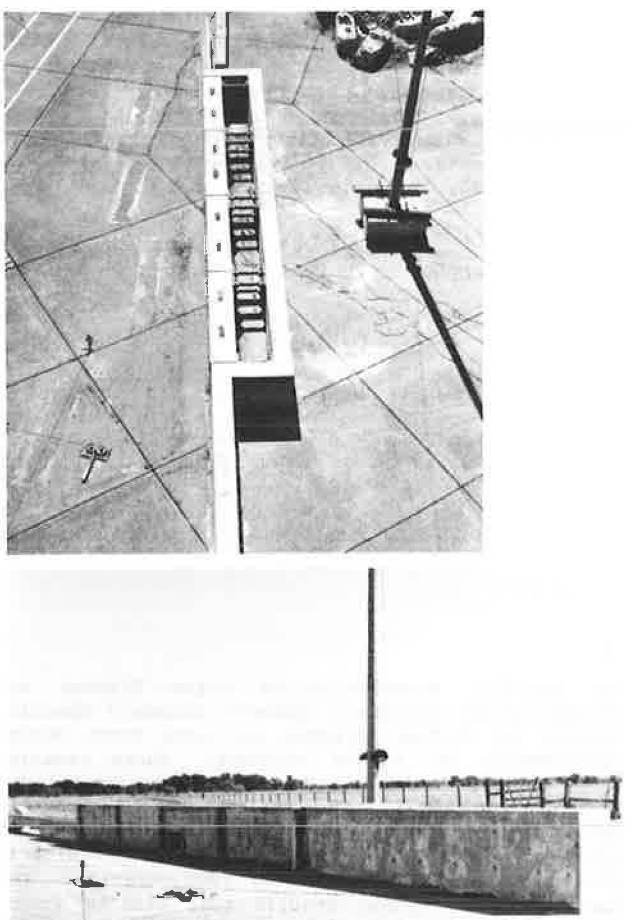

**Figure 2. Measured data from test that used 4740-lb vehicle, 59.9 mph, and 24.0°.**

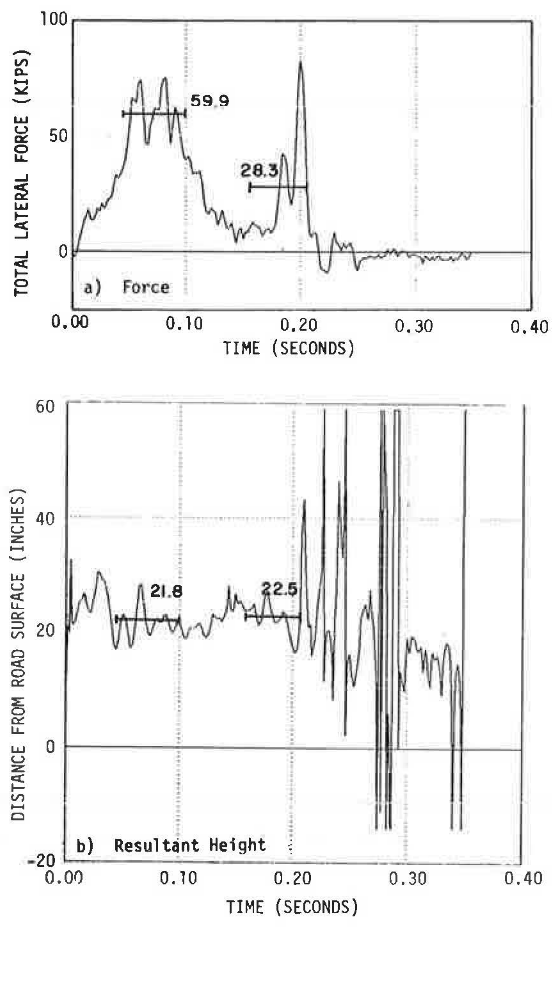

Figure 3. Measured data from test that used 20 030-lb vehicle, 57.6 mph, and 15.0°.

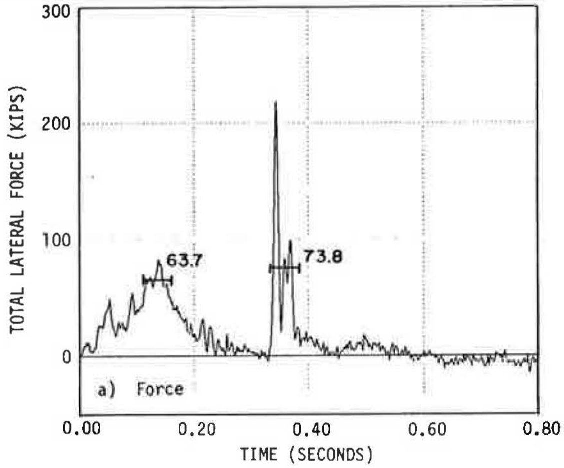


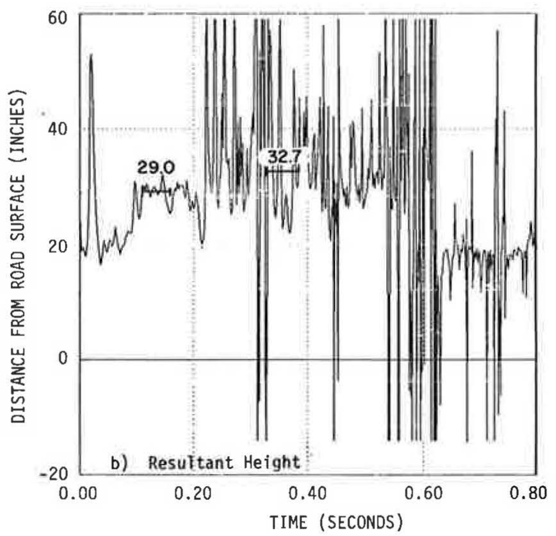


Figure 4. Measured data from test that used 32 020-lb vehicle, 60.0 mph, and 15.0°.

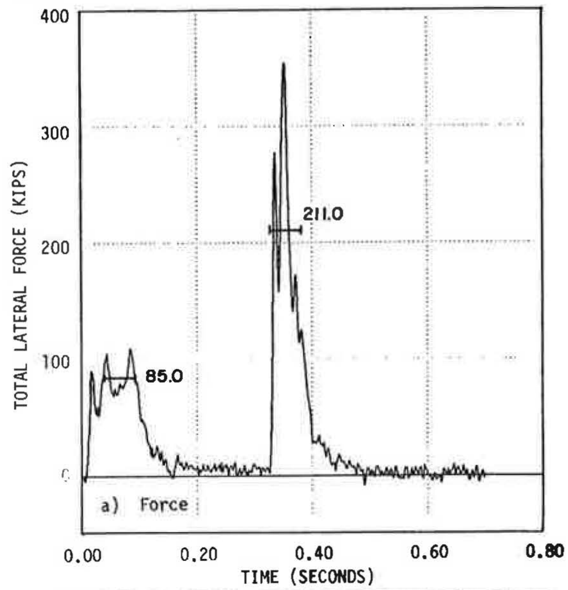


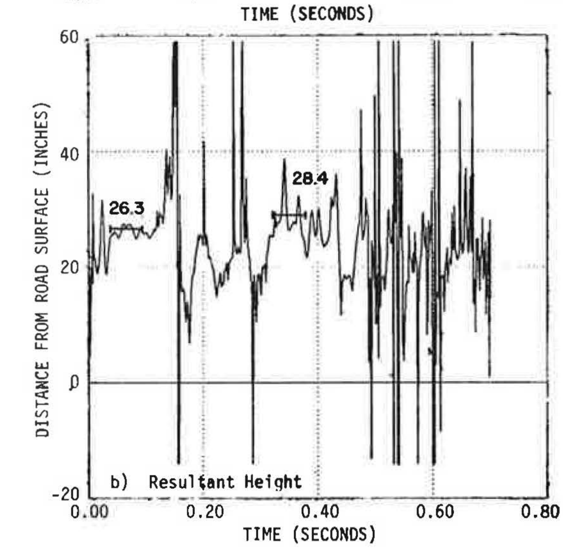


Figure 5. Distribution of contact pressures.

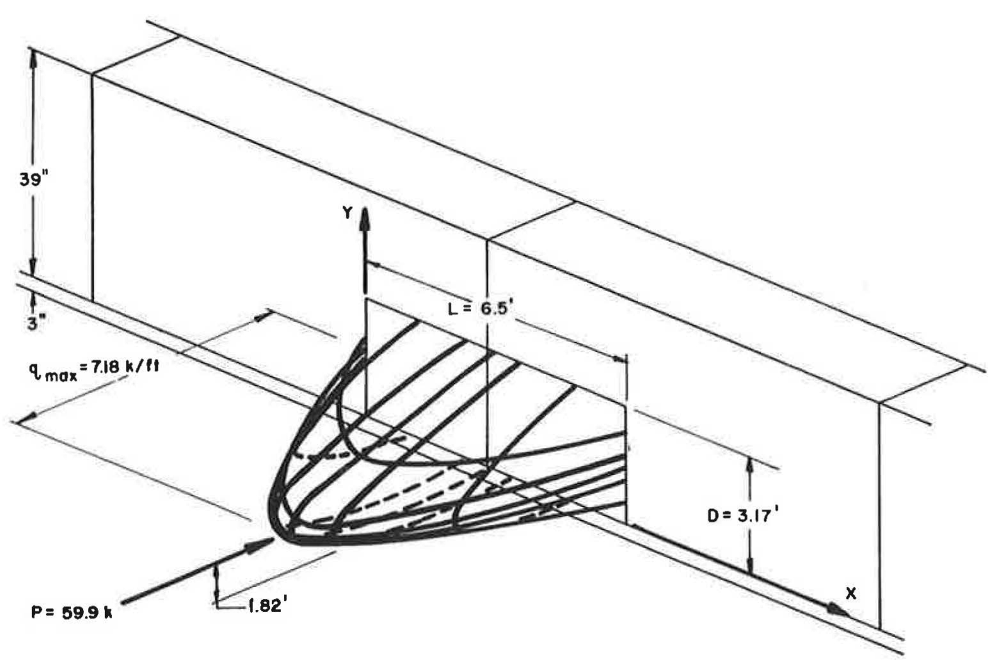

**Figure 6. Longitudinal distribution for initial impact (top) and final impact (bottom) of 4740-lb vehicle at 59.9 mph and 24.0°.**

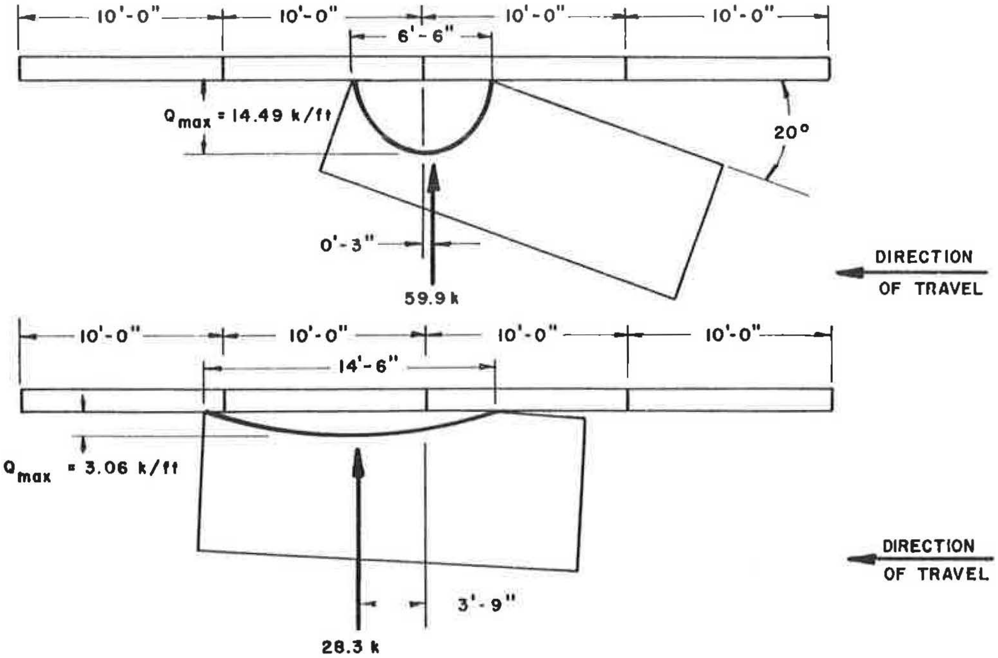


**Table 1. Distribution of forces calculated from the instrumented-wall tests.**

| Test Condition | | | | Resultant | | | | Maximum Force (kips/ft$^2$) | |
|---|---|---|---|---|---|---|---|---|---|
| Weight (lb) | Speed (mph) | Angle (°) | Impact Phase | Height (in) | Magnitude (kips) | Contact Height (ft) | Contact Length (ft) | Per Unit Area | Per Unit Length |
| 2 050 | 59.0 | 15.5 | Initial | 17.0 | 18.4 | 2.33 | 5.0 | 3.89 | 5.76 |
| | | | Final | 18.7 | 8.4 | 2.58 | 7.6 | 1.11 | 1.82 |
| 2 090 | 58.5 | 21.0 | Initial | 19.0 | 21.1 | 2.67 | 6.0 | 3.25 | 5.52 |
| | | | Final | 20.7 | 13.1 | 3.00 | 8.0 | 1.35 | 2.58 |
| 2 800 | 58.3 | 15.0 | Initial | 18.1 | 18.5 | 2.50 | 5.0 | 3.85 | 5.81 |
| | | | Final | 15.3 | 13.9 | 2.08 | 10.8 | 1.82 | 2.01 |
| 2 830 | 56.0 | 18.5 | Initial | 19.3 | 22.0 | 2.92 | 4.8 | 3.65 | 7.61 |
| | | | Final | 21.3 | 22.5 | 3.00 | 10.2 | 1.52 | 3.48 |
| 4 680 | 52.9 | 15.0 | Initial | 21.4 | 52.5 | 3.08 | 7.3 | 5.73 | 11.24 |
| | | | Final | 24.0 | 28.3 | 3.25 | 10.7 | 2.01 | 4.16 |
| 4 740 | 59.9 | 24.0 | Initial | 21.8 | 59.9 | 3.17 | 6.5 | 7.18 | 14.49 |
| | | | Final | 22.5 | 28.3 | 3.25 | 14.5 | 1.48 | 3.06 |
| 20 030 | 57.6 | 15.0 | Initial | 29.0 | 63.7 | 2.17 | 12.3 | 5.88 | 8.12 |
| | | | Final | 32.7 | 73.8 | 1.58 | 25.5 | 4.51 | 4.54 |
| 32 020 | 60.0 | 15.0 | Initial | 26.3 | 85.0 | 2.58 | 6.3 | 12.90 | 21.20 |
| | | | Final | 28.4 | 211.0 | 2.25 | 15.0 | 15.40 | 22.10 |

Three examples of these resultant forces averaged over two 0.05-s intervals are shown in Figures 2a, 3a, and 4a for the impacts of the 4500-lb sedan, the school bus, and the intercity bus, respectively. Figures 2b, 3b, and 4b show the resultant heights during the same time intervals.

Definition of the manner in which the resultant forces are assumed to be distributed over the contact area also required engineering judgments. It was considered obvious that bearing pressure was present at all points of contact between the vehicle and the wall. It was equally obvious that the largest pressures by far were where the elements of the vehicle frame, especially the wheels, made contact with the wall. To include all these considerations in determining the pressure distribution seemed unduly complex. So, to simplify, it was decided to distribute the pressure as one-half a sine wave in both the horizontal and vertical directions. This consideration yielded the following equation:

$$R = \int_0^D \int_0^L q_{max} \sin(\pi x/L) \sin(\pi y/D)\, dy dx \quad (1)$$

where $q_{max}$ is the maximum bearing intensity in kips per square foot, R is the resultant force in kips, and the coordinates x and y and the dimensions L and D (all in feet) of the rectangular contact area are shown in Figure 5. [To calculate the magnitude of the maximum pressure between the vehicle and the wall, the following equation was used: $q_{max}$ = (59.9 kips) $(\pi^2/4DL)$ = 7.16 kips/ft$^2$.] The length of the contact area was measured from the plan-view movie frame that fell nearest the center of each 0.05-s time interval (for both the initial and the final impacts).

An example of how these two frames looked (in this instance for the 4500-lb vehicle that impacted at 24°) and how the longitudinal distributions of contact pressure were deduced from them is indicated by Figure 6 (top and bottom). The depth dimension was deduced by subtracting the 3-in sill height (see Figure 5) from the height of the resultant to find D/2 or, when the resultant lay above (39/2) + 3 = 22.5 in (the mid height of the wall panels), by subtracting the resultant height from 42 in to find D/2. After integration and inversion to solve for the maximum intensity in terms of the measured resultant, one finds that $q_{max} = R\ (\pi^2/4DL)$. The double-sine distribution for the initial impact of the 4740-lb vehicle at 59.9 mph and 24° is shown in Figure 5.

A summary of results from all tests is given in Table 1. Data for both the initial and the final phases of the impact are given for each test. The column headed Height gives the distance from the pavement surface to the resultant impact force, whereas the column headed Contact Height gives the vertical dimension over which the force was distributed. Similarly, the contact length is the distance along the railing over which the force was distributed. These values were used to derive the data in the last two columns, which contain peak values (for the half-sine-wave distribution) of force per unit area and per unit length.

It should be noted that the force measurements were obtained from a nondeflecting barrier and represent the upper bound of forces that would be expected on service railings. Tests conducted on service railings that had typical deflection capabilities result in forces significantly lower than those shown in Table 1.

REFERENCE

1. Standard Specifications for Highway Bridges, 11th ed. AASHTO, Washington, DC, 1973.

*Publication of this paper sponsored by Committee on Safety Appurtenances.*

# Strength of Fillet Welds in Aluminum Lighting Poles

JAMES S. NOEL, C.E. BUTH, AND T.J. HIRSCH

**Tests were performed to ascertain the inherent strength of aluminum fillet welds such as those used to make lighting support poles for highways. It was found that two sources of excess strength beyond that recognized by current design specifications were often available. One was that the strength of a fillet weld when loaded so that the resultant forces are perpendicular to its length is 35-45 percent greater than when it is loaded parallel to its length. The other, applicable only to members that are hollow and round or near-round (as are virtually all the aluminum highway lighting support poles), was that the shape factor for such cross sections was 1.31 rather than 1.12, the shape factor often used for most metal structural shapes. Examples of a near-round member include many-sided polygons and ellipses in which the major and minor axes are nearly the same length. Because the shape factor represents excess strength beyond first yield, this finding represents a [(1.31/1.12) - 1] 100 percent = 17 percent increase in load-carrying capacity. A method is suggested for amending the applicable specifications to reflect these greater strengths.**

Weld sizes used by manufacturers of spun-aluminum lighting poles were established primarily on the basis of tests conducted by the individual companies. Although experience has shown that these weld sizes are satisfactory, both state and federal highway engineers have questioned whether they can be justified by using only the requirements of the American Association of State Highway and Transportation Officials (AASHTO) (1).

The AASHTO specifications refer to the Aluminum Association's Specifications for Aluminum Bridge and Other Highway Structures (2), which calls for an allowable shear stress of 30 MPa in fillet welds of filler alloy 4043 with parent alloy 6063. This allowable stress was established on the basis of longitudinal shear stress tests of fillet welds and a bridge safety factor of 2.64.

The geometry at the base of most aluminum highway support poles is similar to that shown in Figure 1. The relatively thin-walled circular pole is connected into a cast-aluminum base flange by a circumferential fillet weld or welds as shown. Bending of the pole by the forces of nature causes the fillet welds to be stressed perpendicular to their lengthwise (circumferential) direction. Part of the purpose of this study was to determine whether an allowable stress greater than 30 MPa should be used because of the difference in strength between transverse and longitudinal loading of fillet welds.

The effect that the circular shape of the weld has on the bending strength of the joint was also included among the objectives. The published allowable stresses for bending of round and elliptical tubes take into account the greater strength of these shapes compared with that of other shapes. But these same effects are not recognized by the allowable stresses prescribed for circumferential welds.

The Tapered Aluminum Pole Group of the National Electrical Manufacturers Association elected to support a program designed to quantify the significance of these effects and, if possible, to suggest how the results could be incorporated into the existing specifications for such structures.

STRENGTH OF TRANSVERSE VERSUS LONGITUDINAL FILLET WELDS

Comparison of the results of the tests of weld splices in flat-bar specimens confirmed what has long been known by structural engineers, namely, that the load-carrying capacity of a fillet weld transverse to the direction of a tensile traction is considerably greater than that of a fillet weld parallel to the traction. Spraragen and Claussen (3) report that tests of fillet welds in the 1920s and 1930s had already determined that transverse fillets would carry up to 40 percent more load than would parallel fillets. Usually this difference in strength is ignored by design specifications, which are predicated on the weakest possible configuration for the weld and load. Associated commentaries and textbooks usually explain that the excess strength is disregarded, primarily to simplify calculations (4).

A simple strength-of-materials approach to demonstrating the excess strength, as opposed to a theory-of-elasticity approach, is quite convincing.